



Adaptive Flight Control with Unknown Time-Varying Unstable Zero Dynamics

Syed Aseem Ul Islam ^{*}, Adam L. Bruce [†], Tam W. Nguyen [‡], Ilya Kolmanovsky [§], and Dennis S. Bernstein [¶]
University of Michigan, Ann Arbor, MI, 48109

This paper develops data-driven retrospective cost adaptive control (DDRCAC). The motivation for this model-free digital adaptive control technique is flight control, where the aircraft undergoes an unknown transition from minimum-phase to nonminimum-phase dynamics.

I. Introduction

IN many applications of flight control, it is extremely difficult, if not impossible, to model the vehicle dynamics with sufficient accuracy for fixed-gain control methods. These applications are candidates for adaptive control [1–3]. The goal of adaptive control is thus to provide reliable stabilization, command following, and disturbance rejection in the presence of high levels of uncertainty in both the vehicle dynamics and exogenous signals.

A longstanding challenge in adaptive control irrespective of the application is the problem of nonminimum-phase (NMP) zeros. Traditional adaptive controllers assume that the plant dynamics are minimum phase. However, longitudinal aircraft dynamics are well known to be NMP.

Retrospective cost adaptive control (RCAC), which is a direct digital adaptive control technique, is applicable to NMP systems [4]. However, as shown in [4], uncertainty in the knowledge of the NMP zeros can lead to NMP pole/zero cancellation, leading to a hidden instability. It is thus of interest to extend RCAC to accommodate uncertainty in NMP zeros of the plant.

The present paper develops an extension of RCAC that overcomes uncertainty in the NMP plant zeros. This approach, called *data-driven RCAC (DDRCAC)*, uses concurrent discrete-time closed-loop system identification in order to elicit the essential modeling information needed by RCAC. The system identification is based on an extension of recursive least squares (RLS) with variable-rate forgetting (VRF). DDRCAC is thus an indirect digital adaptive control technique. Since DDRCAC, like RCAC, is a digital control technique, it can take advantage of modeling information obtained by discrete-time system identification at the specified sample rate, it need not account separately for delays and phase shifts due to sample and hold operations, and it avoids the need for controller discretization.

The goal of the present paper is to apply DDRCAC to the plants that undergo an unknown transition from minimum-phase to NMP dynamics. In particular, DDRCAC is used to follow step and harmonic commands in the presence of an unknown transition from MP to NMP. This problem is motivated by flight control for a hypersonic aircraft model that transitions from MP to NMP [5–13]. RCAC was earlier applied to this problem in [14, 15] with the time of the transition from MP to NMP dynamics known. The assumption that the onset time is known is not realistic under real-world flight conditions, where the onset time and details of the transition would be unknown. Consequently, no knowledge of the transition from MP to NMP dynamics is used in this paper.

Related studies on modeling and control of hypersonic vehicles with NMP zero dynamics are given in [11, 16–18]. Models of hypersonic aircraft are given in [1–3, 5, 18, 19]. These models are valid for small operating envelopes and are typically difficult to verify experimentally. These challenges motivate the need for control techniques that are data-driven and model free.

The contents of this paper are as follows. Section II describes the control architecture on which this paper is based. In section III we present the DDRCAC algorithm. Section IV presents illustrative toy examples that demonstrate DDRCAC on a SISO and SIMO plant that undergo an unknown transition from MP to NMP dynamics. Finally, section V applies DDRCAC to a model of a hypersonic aircraft that undergoes an unknown MP to NMP transition.

^{*}Graduate Student, Aerospace Engineering, 1320 Beal Ave, Ann Arbor, MI, USA.

[†]Graduate Student, Aerospace Engineering, 1320 Beal Ave, Ann Arbor, MI, USA.

[‡]Post-Graduate Researcher, Aerospace Engineering, 1320 Beal Ave, Ann Arbor, MI, USA.

[§]Professor, Aerospace Engineering, 1320 Beal Ave, Ann Arbor, MI, USA.

[¶]Professor, Aerospace Engineering, 1320 Beal Ave, Ann Arbor, MI, USA.

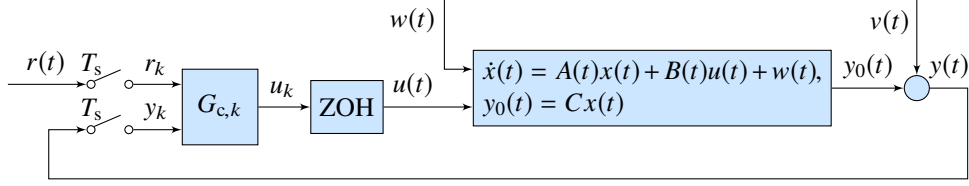


Fig. 1 Basic servo loop for the control of continuous-time, time-varying dynamics, where the measurement $y(t)$ is the true measurement $y_0(t)$ corrupted by sensor noise $v(t)$. The disturbance $w(t)$ may not be matched with the control $u(t)$. The sampled command r_k and measurement y_k are the inputs to the controller $G_{c,k}$, which is adaptively updated at each time step. The controller produces u_k , which is operated upon by a zero-order hold to produce the continuous-time control $u(t)$.

II. Control Architecture

Consider the continuous-time, time-varying system

$$\dot{x}(t) = A(t)x(t) + B(t)u(t) + w(t), \quad (1)$$

$$y(t) = Cx(t) + v(t), \quad (2)$$

where $x(t) \in \mathbb{R}^n$, $A(t) \in \mathbb{R}^{n \times n}$, $B(t) \in \mathbb{R}^{n \times m}$, $u(t) \in \mathbb{R}^m$, $w(t) \in \mathbb{R}^n$, $y(t) \in \mathbb{R}^p$, $C \in \mathbb{R}^{p \times n}$, and $v(t) \in \mathbb{R}^p$. Equations (1), (2) are defined to be the system G . The objective is to follow step and harmonic commands $r(t) \in \mathbb{R}^p$ asymptotically using the architecture shown in Figure 1. As shown in Figure 1, $w(t)$ and $v(t)$ are continuous-time stochastic signals. We do not specify the stochastic properties of these signals. Instead, we specify the properties of the corresponding sampled signals w_k and v_k , respectively [20–22]. The system (1), (2) is simulated using the ode45 solver in Matlab between the controller sample periods. The sampled signals are defined as

$$r_k \triangleq r(kT_s), \quad y_k \triangleq y(kT_s), \quad u_k \triangleq u(kT_s), \quad w_k \triangleq w(kT_s), \quad v_k \triangleq v(kT_s), \quad (3)$$

where k is the number of samples, and T_s is the sampling period. We define the command-following error as

$$z_k \triangleq r_k - y_k \in \mathbb{R}^p, \quad (4)$$

where $r_k \in \mathbb{R}^p$ is the sampled command.

III. Data-Driven Retrospective Cost Adaptive Control

DDRCAC consists of two components, namely, online identification and RCAC. The online identification uses RLS to fit an IIR IO model using y_k and u_k data obtained during closed-loop operation. A second implementation of RLS is used to update the RCAC adaptive controller using a target model constructed from the latest identified model. In particular, at each step we construct the target model $G_{t,k}$ as an FIR filter whose numerator is identical to the numerator of the latest identified IIR model. Both RLS implementations use data-dependent variable-rate forgetting (VRF). The following result is RLS with VRF that is used to implement DDRCAC.

Proposition 1 For all $k \geq 0$, let $Y_k \in \mathbb{R}^{l_y}$, $\Phi_k \in \mathbb{R}^{l_y \times l_\theta}$, $\lambda_k \in (0, 1]$, and define $\rho_k \triangleq \prod_{j=0}^k \lambda_j$. Let $\Theta_0 \in \mathbb{R}^{l_\theta}$, and let $P_0 \in \mathbb{R}^{l_\theta \times l_\theta}$ be positive definite. Furthermore, for all $k \geq 0$, denote the minimizer of the function

$$J_k(\Theta) \triangleq \sum_{i=0}^k \frac{\rho_k}{\rho_i} (Y_i - \Phi_i \Theta)^T (Y_i - \Phi_i \Theta) + \rho_k (\Theta - \Theta_0)^T P_0^{-1} (\Theta - \Theta_0). \quad (5)$$

where $\Theta \in \mathbb{R}^{l_\theta}$, by $\Theta_{k+1} \triangleq \underset{\Theta \in \mathbb{R}^{l_\theta}}{\operatorname{argmin}} J_k(\Theta)$. Then, for all $k \geq 0$, Θ_{k+1} is given by

$$P_{k+1} = \frac{1}{\lambda_k} P_k - \frac{1}{\lambda_k} \Phi_k^T (\lambda_k I_{l_y} + \Phi_k P_k \Phi_k^T)^{-1} \Phi_k P_k, \quad (6)$$

$$\Theta_{k+1} = \Theta_k + P_{k+1} \Phi_k^T (Y_k - \Phi_k \Theta_k). \quad (7)$$

A. Online Identification

We fit a strictly-proper linear IO model of the form

$$y_k = - \sum_{i=1}^{\eta} F_{i,k} y_{k-i} + \sum_{i=1}^{\eta} G_{i,k} u_{k-i}, \quad (8)$$

to y_k and u_k , where η is the model window length, $F_i \in \mathbb{R}^{p \times p}$ and $G_i \in \mathbb{R}^{p \times m}$ are the model coefficient matrices that are to be updated. To perform this update recursively we define the plant identification error

$$z_{p,k}(\theta_p) \triangleq y_k - \phi_{p,k} \theta_p, \quad (9)$$

where

$$\phi_{p,k} \triangleq \begin{bmatrix} -y_{k-1} \\ \vdots \\ -y_{k-\eta} \\ u_{k-1} \\ \vdots \\ u_{k-\eta} \end{bmatrix}^T \otimes I_p \in \mathbb{R}^{p \times l_{\theta_p}}, \quad \theta_{p,k} \triangleq \text{vec} [F_{1,k} \cdots F_{\eta,k} \ G_{1,k} \cdots G_{\eta,k}] \in \mathbb{R}^{l_{\theta_p}}, \quad (10)$$

and $l_{\theta_p} \triangleq \eta p(p+m)$. The cost (5) with $Y_k - \Phi_k \Theta = z_{p,k}(\theta_p)$ is minimized using Proposition 1 with

$$Y_k \triangleq y_k, \quad \Phi_k \triangleq \phi_{p,k}, \quad \Theta \triangleq \theta_p, \quad \lambda_k \triangleq \lambda_{p,k}, \quad (11)$$

which recursively produces the minimizer $\theta_{p,k+1}$.

B. Retrospective Cost Adaptive Control

Define the dynamic compensator

$$u_k \triangleq \text{sat}_{\alpha}(\phi_k \theta_k), \quad (12)$$

where

$$\phi_k \triangleq \begin{bmatrix} u_{k-1} \\ \vdots \\ u_{k-n_c} \\ y_{k-1} \\ \vdots \\ y_{k-n_c} \end{bmatrix}^T \otimes I_m \in \mathbb{R}^{m \times l_{\theta}}, \quad (13)$$

n_c is the controller window length, $l_{\theta} = n_c m(m+p)$, and θ_k is a vector of controller coefficients to be optimized. With the definition (13) of ϕ_k , (12) represents an IIR controller whose output is saturated by a multivariable saturation function sat_{α} . In particular, each entry x_i of a vector x is independently saturated by the corresponding entry α_i of α , to produce each entry $\text{sat}_{\alpha_i}(x_i)$ of $\text{sat}_{\alpha}(x)$. That is

$$\text{sat}_{\alpha_i}(x_i) \triangleq \begin{cases} x_i, & |x_i| < \alpha_i, \\ \text{sign}(x_i) \alpha_i, & |x_i| \geq \alpha_i. \end{cases} \quad (14)$$

Next, define the retrospective cost variable

$$\hat{z}_k(\theta) \triangleq \begin{cases} \begin{bmatrix} z_k + N_k \bar{\phi}_k \theta - N_k \bar{U}_k \end{bmatrix} \in \mathbb{R}^p, & R_u = 0, \\ \begin{bmatrix} z_k + N_k \bar{\phi}_k \theta - N_k \bar{U}_k \\ R_u(u_{\alpha,k+1} - \phi_k \theta) \end{bmatrix} \in \mathbb{R}^{p+m}, & R_u \neq 0, \end{cases} \quad (15)$$

where

$$\bar{\phi}_k \triangleq \begin{bmatrix} \phi_{k-1} \\ \vdots \\ \phi_{k-\eta} \end{bmatrix} \in \mathbb{R}^{\eta m \times l_\theta}, \quad \bar{U}_k \triangleq \begin{bmatrix} u_{k-1} \\ \vdots \\ u_{k-\eta} \end{bmatrix} \in \mathbb{R}^{\eta m}, \quad (16)$$

$$N_k \triangleq \begin{cases} [-1_{p \times m} \ 0 \ \cdots \ 0] & G_{i,k+1} = 0, \\ [-G_{1,k+1} \ \cdots \ -G_{\eta,k+1}] & \text{otherwise,} \end{cases} \quad (17)$$

$$z_k \triangleq r_k - y_k, \quad (18)$$

$R_u \in \mathbb{R}^{m \times m}$ positive-semidefinite is the control weight, $G_{i,k+1} \in \mathbb{R}^{p \times m}$ for $i = 1, \dots, \eta$ are the numerator coefficients of the identified model, $N_k \in \mathbb{R}^{p \times \eta m}$, $r_k \in \mathbb{R}^p$ is the command, and $z_k \in \mathbb{R}^p$ is the command-following error and the adaptation variable. Note that the identification update at step k can be performed before the adaptive control update and thus $G_{i,k+1}$ are available for the construction of N_k at step k . The cost (5) with $Y_k - \Phi_k \Theta = \hat{z}_k(\theta)$ is minimized using Proposition 1 with

$$Y_k \triangleq \begin{cases} z_k - N_k \bar{U}_k \in \mathbb{R}^p, & R_u = 0, \\ \begin{bmatrix} z_k - N_k \bar{U}_k \\ 0 \end{bmatrix} \in \mathbb{R}^{p+m}, & R_u \neq 0, \end{cases} \quad (19)$$

$$\Phi_k \triangleq \begin{cases} -N_k \bar{\phi}_k \in \mathbb{R}^{p \times l_\theta}, & R_u = 0, \\ \begin{bmatrix} -N_k \bar{\phi}_k \\ R_u \phi_k \end{bmatrix} \in \mathbb{R}^{(p+m) \times l_\theta}, & R_u \neq 0, \end{cases} \quad (20)$$

$$\Theta \triangleq \theta, \quad \lambda_k \triangleq \lambda_{c,k}, \quad (21)$$

which recursively produces the minimizer θ_{k+1} .

For all examples in this paper, $\theta_{p,k}$ and θ_k are initialized as 0 in order to reflect the absence of additional prior modeling information. In addition, for both implementations of RLS $P_0 = p_0 I_{l_\theta}$ where p_0 is a positive number to be selected.

C. Data-Dependent Variable Rate Forgetting

To implement data-dependent variable-rate forgetting, we define

$$\lambda_{p,k} \triangleq \frac{1}{1 + \gamma f_{\tau_1, \tau_2, k}[z_{p,k}(\theta_{p,k})]}, \quad \lambda_{c,k} \triangleq \frac{1}{1 + \gamma f_{\tau_1, \tau_2, k}(z_k)}, \quad (22)$$

which are the time-varying data-dependent plant-identification and control forgetting factors, respectively, where

$$f_{\tau_1, \tau_2, k}(x_k) \triangleq \begin{cases} \frac{\xi_n}{\xi_d} - 1, & \frac{\xi_n}{\xi_d} > 1, \\ 0, & \frac{\xi_n}{\xi_d} \leq 1 \text{ or } \xi_d = 0, \end{cases} \quad \xi_n \triangleq \left(\frac{1}{\tau_1} \sum_{i=k-\tau_1}^k x_i^T x_i \right)^{1/2}, \quad \xi_d \triangleq \left(\frac{1}{\tau_2} \sum_{i=k-\tau_2}^k x_i^T x_i \right)^{1/2}, \quad (23)$$

x_k is a vector and $\tau_1 < \tau_2$ are integers. The terms ξ_n and ξ_d are the average norms of x_k over periods of length τ_1 and τ_2 , respectively. The integer τ_2 is chosen to be large so that ξ_d approximates the long-term variation of the x_k , whereas τ_1 is chosen to be small so that ξ_n approximates the short-term variation of the x_k . Consequently, the case $\frac{\xi_n}{\xi_d} > 1$ implies that the variation of x_k is greater in the recent past than over a longer time interval. The function f is used in DDRCAC to suspend forgetting when the variation of the error drops below a threshold determined by the ratio $\frac{\xi_n}{\xi_d}$. This technique thus prevents DDRCAC from forgetting due to sensor noise rather than due the magnitude of the noise-free command-following error.

A list of parameters to be selected for DDRCAC is presented in Table 1.

Parameter	Description	Selection
η	Model window length	Integer ≥ 1
n_c	Controller window length	Integer ≥ 1
R_u	Control weight	0 or $r_u I_m, r_u > 0$
α	Control saturation level vector	Actuator saturation
p_0	Initial RLS covariance scaling	$p_0 > 0$
γ	Forgetting parameter	$0 \leq \gamma < 1$
τ_1, τ_2	Forgetting window lengths	Integers $\tau_2 > \tau_1$

Table 1 Tuning parameters that need to be selected for DDRCAC.

IV. Illustrative Examples

Example 1. Harmonic command following for a single-input single-output system with unknown transition from MP to NMP. Consider the continuous-time system given by (1), (2) with

$$A(t) = \begin{bmatrix} \ell(t, -0.2, -0.1) & \ell(t, -2, -4) \\ \ell(t, 2, 4) & 0 \end{bmatrix}, \quad B(t) = \begin{bmatrix} \ell(t, -1, 1) \\ \ell(t, 0.1, 0) \end{bmatrix}, \quad (24)$$

$$C = \begin{bmatrix} 1 & -0.025 \end{bmatrix}, \quad \ell(t, a, b) \triangleq \begin{cases} a, & t < t_1, \\ a + \frac{t-t_1}{t_2-t_1}(b-a), & t_1 \leq t \leq t_2, \\ b, & t > t_2, \end{cases} \quad (25)$$

and $t_1 = 40$ s, $t_2 = 50$ s. The command is given by

$$r(t) = \begin{cases} 6 \sin 1.3t, & t < 80 \text{ s}, \\ 9 \sin 2.1t, & t \geq 80 \text{ s}. \end{cases} \quad (26)$$

The sequences w_k and v_k are zero-mean Gaussian with covariances $0.0001^2 I_2$ and 0.001^2 , respectively. The instantaneous poles and zeros of G as a function of t are shown in Figure 2. The real MP zero moves towards $-\infty$, reappears at $+\infty$, and converges to a point in the open-right half plane. The lightly damped poles move closer to the imaginary axis.

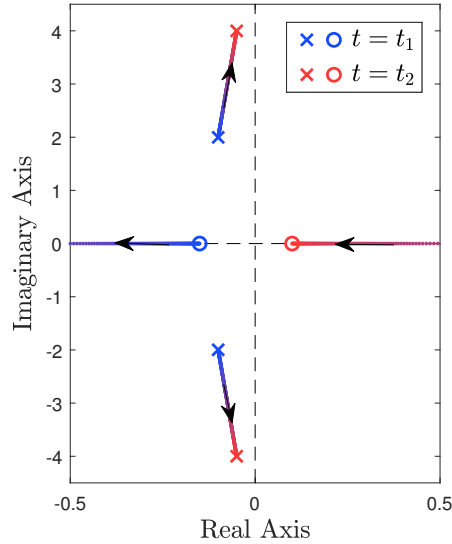


Fig. 2 Example 1: Locations of the instantaneous poles and zeros of G during the transition from t_1 to t_2 . The system transitions from MP to NMP, as shown by the minimum-phase zero that starts in the open-left half plane, approaches $-\infty$, reappears at $+\infty$, and converges to a point in the open-right half plane.

To apply DDRCAC we set $T_s = 0.1$ s, $\eta = 8$, $n_c = 10$, $p_0 = 1000$, $R_u = 0$, $\gamma_p = \gamma_c = 0.1$, $\alpha = 90$, $\tau_1 = 40$, and $\tau_2 = 200$. Figure 3 shows that asymptotic harmonic command following is achieved for a harmonic command that abruptly changes frequency at $t = 80$ s. Figure 4 shows the numerator and denominator coefficients of the identified model and the plant identification forgetting factor $\lambda_{p,k}$. Figure 5 shows the numerator and denominator coefficients of the adaptive controller and the control forgetting factor $\lambda_{c,k}$. $\lambda_{p,k}$ and $\lambda_{c,k}$ fall below their maximum value of 1 for the initial adaptation, the MP to NMP transition of G , and the command frequency change. The unknown transition from MP to NMP is marked with red shaded regions in Figures 3–5. \diamond

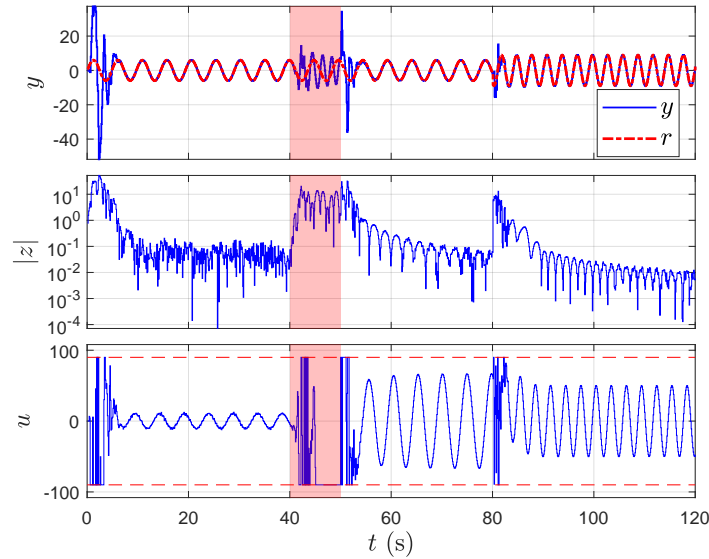


Fig. 3 Example 1: Harmonic command following with an unknown transition from MP to NMP dynamics.

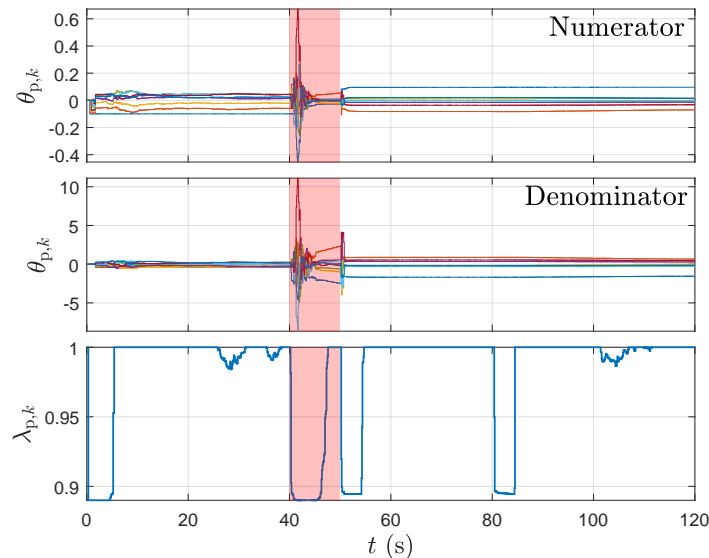


Fig. 4 Example 1: Numerator and denominator coefficients of the identified model, and the plant identification forgetting factor $\lambda_{p,k}$. Forgetting occurs for initial adaptation, the transition from MP to NMP, and the change in command frequency.

Example 2. Multi-step command following for a single-input multiple-output system with unknown transition from

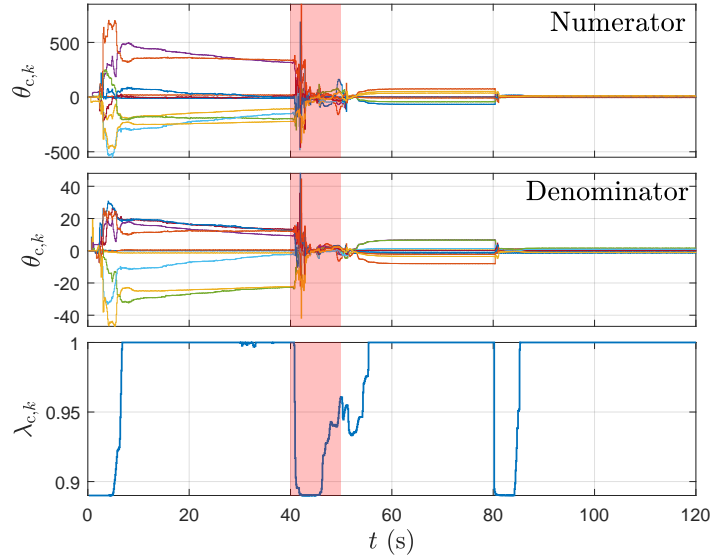


Fig. 5 Example 1: Numerator and denominator coefficients of the adaptive controller, and the control forgetting factor $\lambda_{c,k}$. Forgetting occurs for initial adaptation, the transition from MP to NMP, and the change in command frequency.

stable MP to unstable NMP. Consider the continuous-time system given by (1), (2) with

$$A(t) = \begin{bmatrix} \ell(t, -0.6, -0.1) & \ell(t, -5, -4) & 0.5 \\ \ell(t, 6, 4) & 0 & \ell(t, -0.1, -0.1) \\ \ell(t, -0.4, -0.1) & \ell(t, -3.7, 0.8) & \ell(t, -0.3, 0.3) \end{bmatrix}, \quad B(t) = \begin{bmatrix} \ell(t, -0.5, 2) \\ \ell(t, -0.05, 0) \\ \ell(t, -0.9, -1) \end{bmatrix}, \quad (27)$$

$$C = \begin{bmatrix} 1 & -0.025 & 0.2 \\ 0.2 & -0.005 & 0.04 \end{bmatrix}, \quad (28)$$

and $t_1 = 75$ s, $t_2 = 95$ s. The command is a sequence of steps of magnitude 10 and -10, each of length 30 s. The sequences w_k and v_k are zero-mean Gaussian with covariances $0.0001^2 I_3$ and 0.001^2 , respectively. The instantaneous poles and transmission zeros of G as a function of t are shown in Figure 6. A pair of complex transmission zeros and a real pole in the left-half plane move to the right-half plane. A pair of complex poles near the imaginary axis changes frequency and damping.

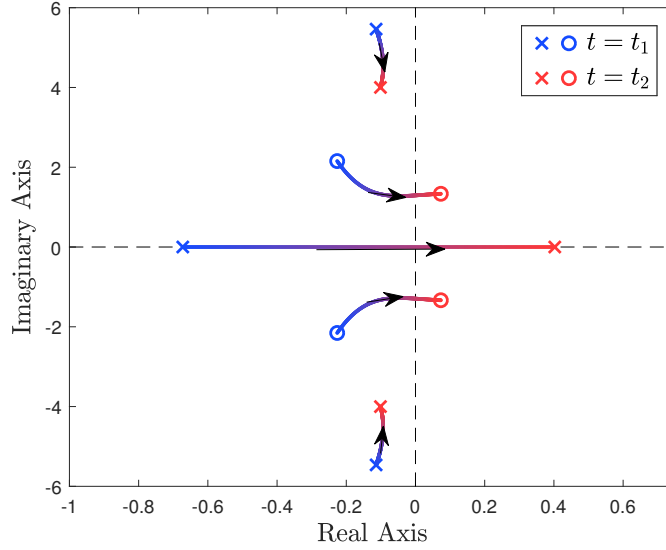


Fig. 6 Example 2: Locations of the instantaneous poles and transmission zeros of the G during the transition from t_1 to t_2 . The system transitions from stable MP to unstable NMP.

To apply DDRCAC we set $T_s = 0.1$ s, $\eta = 8$, $n_c = 10$, $p_0 = 1000$, $R_u = 0$, $\gamma_p = \gamma_c = 0.1$, $\alpha = 90$, $\tau_1 = 40$, and $\tau_2 = 200$. Figure 3 shows that asymptotic multi-step command following is achieved. Figure 4 shows the numerator and denominator coefficients of the identified model and the plant identification forgetting factor $\lambda_{p,k}$. Figure 5 shows the numerator and denominator coefficients of the adaptive controller and the control forgetting factor $\lambda_{c,k}$. $\lambda_{p,k}$ and $\lambda_{c,k}$ fall below their maximum value of 1 for the initial adaptation, the MP to NMP transition of G , and the changes in sign of the command. The unknown transition from stable MP to unstable NMP is marked with red shaded regions in Figures 7–9. \diamond

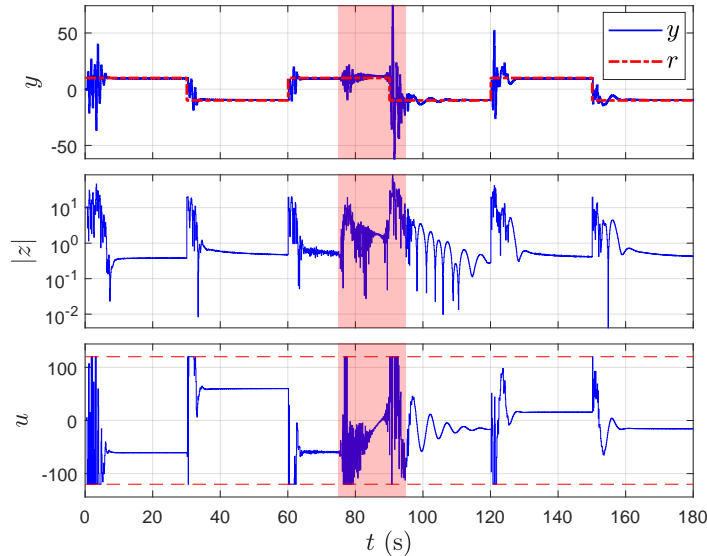


Fig. 7 Example 2: Multi-step command following with an unknown transition from stable MP to unstable NMP dynamics.

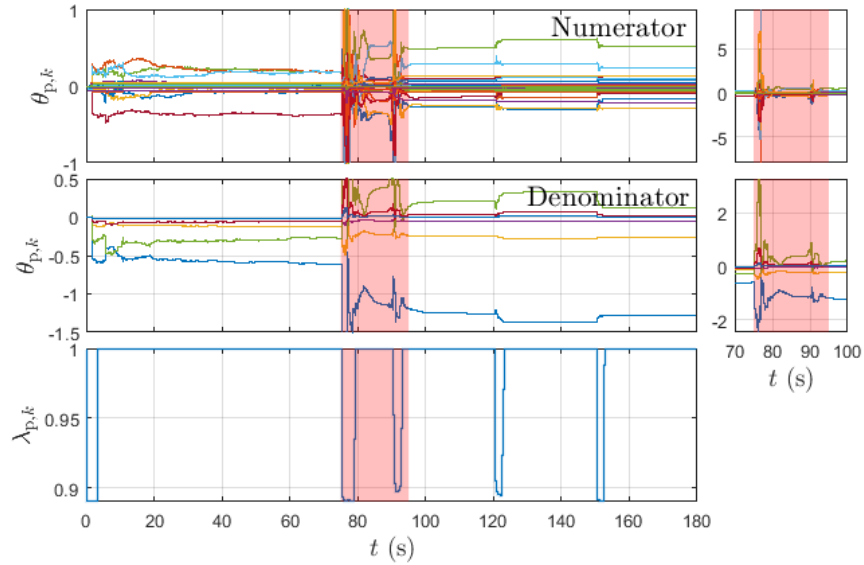


Fig. 8 Example 2: Numerator and denominator coefficients of the identified model, and the plant identification forgetting factor $\lambda_{p,k}$. The numerator and denominator coefficient plots are clipped and the unclipped sections of the plot are shown as inserts on the right. Forgetting occurs for initial adaptation, the transition from stable MP to unstable NMP, and the change in the sign of the step command. Forgetting in response to change in sign of step command occurs only when G is unstable and NMP.

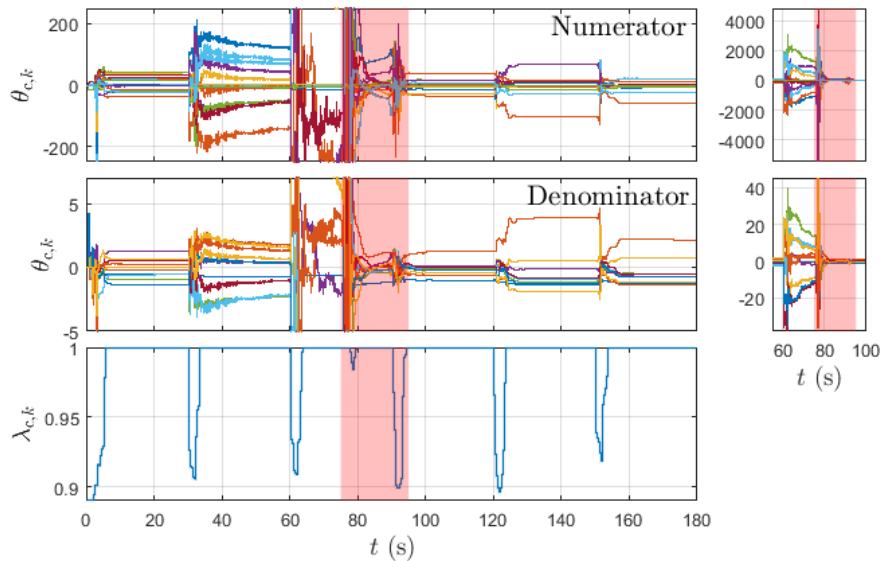


Fig. 9 Example 2: Numerator and denominator coefficients of the adaptive controller, and the control forgetting factor $\lambda_{c,k}$. The numerator and denominator coefficient plots are clipped and the unclipped sections of the plot are shown as inserts on the right. Forgetting occurs for initial adaptation, the transition from stable MP to unstable NMP, and the change in the sign of the step command.

V. Lateral Dynamics of a Hypersonic Aircraft that transitions from MP to NMP

We consider a model, which is a 4th-order single-input single-output (SISO) linearization of the vehicle's lateral dynamics, which transitions from MP to NMP zero dynamics. This model is given by (1), (2) with

$$A(t) \triangleq \begin{bmatrix} -0.0771 & 0.269 & -0.9631 & 0.0397 \\ \ell(t, -25.6, -108.8) & 0.0218 & 0.0995 & 0 \\ \ell(t, 0.6160, 0.4107) & 0.0376 & -0.2687 & 0 \\ 0 & 1 & 0.4202 & 0.0058 \end{bmatrix}, \quad B(t) \triangleq \begin{bmatrix} -0.0002 \\ 2.519 \\ \ell(t, -0.0222, -0.0665) \\ 0 \end{bmatrix}, \quad (29)$$

$$C \triangleq \begin{bmatrix} 0 & 0 & 0 & 1 \end{bmatrix}, \quad (30)$$

and the components of $x \triangleq \begin{bmatrix} \beta & p & r & \phi \end{bmatrix}^T$ are sideslip angle in rad, body x -axis angular velocity in rad/s, body z -axis angular velocity in rad/s, and roll angle in rad. The instantaneous poles and zeros of this model as a function of t are shown in Figure 10. The signal $u(t) = \delta_a(t)$ represents the asymmetric deflection of the split flaps in rad. For realism, we implement actuator rate and magnitude saturations at 300 deg/s and 30 deg, respectively. The sequences w_k and v_k are zero-mean Gaussian with covariances $0.0001^2 I_4$ and 0.001^2 , respectively.

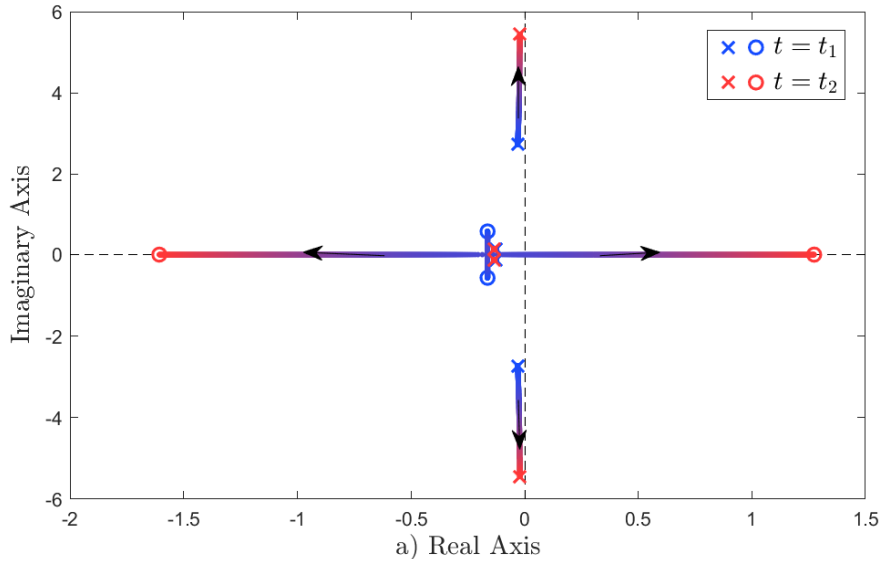


Fig. 10 Instantaneous poles and zeros of the hypersonic aircraft model during the transition from t_1 to t_2 . A pair of complex MP zeros transition to one real MP and one real NMP zero. A pair of complex lightly-damped poles moves closer to the imaginary axis and increase in frequency. Under real-world operational flight conditions, the onset of the transition and its time-dependence are unknown.

Example 3. *Multi-step command following for a hypersonic aircraft with an unknown transition from MP to NMP.* Consider the continuous-time system given by (1), (2) with (29), (30) and $t_1 = 90$ s, $t_2 = 100$ s. The times t_1, t_2 are not known to the control algorithm. The roll-angle command is

$$r(t) = \begin{cases} 10 \sin 1.3t \text{ deg}, & t < 100 \text{ s}, \\ 15 \sin 2.1t \text{ deg}, & t \geq 100 \text{ s}. \end{cases} \quad (31)$$

To apply DDRCAC we set $T_s = 0.5$ s, $\eta = 8$, $n_c = 10$, $p_0 = 1000$, $R_u = 0$, $\gamma_p = \gamma_c = 0.1$, $\alpha = 30$ deg, $\tau_1 = 40$, and $\tau_2 = 200$. Figure 11 shows that asymptotic harmonic command following is achieved. Figure 12 shows the numerator and denominator coefficients of the identified model and the plant identification forgetting factor $\lambda_{p,k}$. Figure 13 shows the numerator and denominator coefficients of the adaptive controller and the control forgetting factor $\lambda_{c,k}$. $\lambda_{p,k}$ and $\lambda_{c,k}$ fall below their maximum value of 1 for the initial adaptation and the MP to NMP transition of the model. The unknown transition from MP to NMP is marked with red shaded regions in Figures 11–13. \diamond

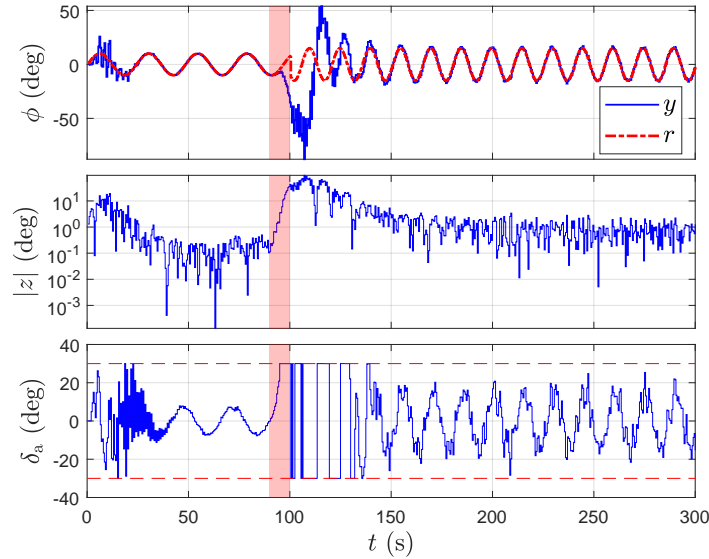


Fig. 11 Example 3: Harmonic command following with an unknown transition from MP to NMP dynamics.

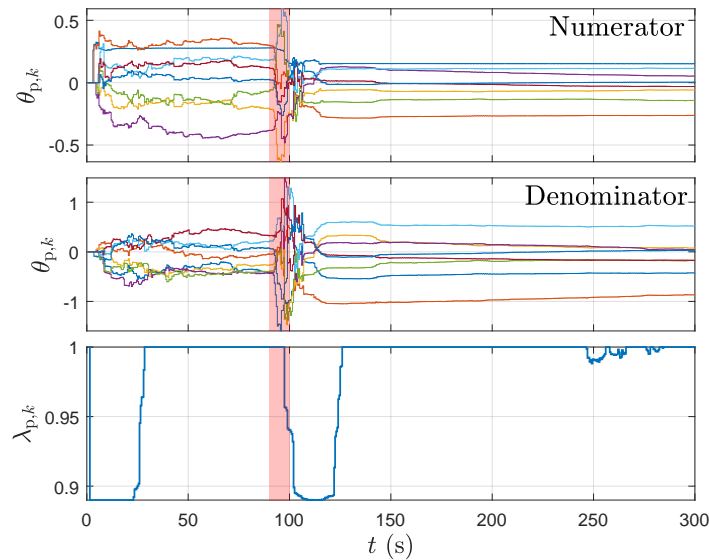


Fig. 12 Example 3: Numerator and denominator coefficients of the identified model, and the plant identification forgetting factor $\lambda_{p,k}$. Forgetting occurs for initial adaptation and the transition from MP to NMP.

VI. Conclusions

This paper demonstrated the application of *data-driven retrospective cost adaptive control (DDRCAC)*, which is an extension of RCAC to include concurrent system identification based on recursive least squares (RLS) with variable-rate forgetting (VRF). The principal motivation for DDRCAC is the problem of controlling time-varying systems that undergo an unknown transition from minimum-phase (MP) to nonminimum-phase (NMP) dynamics. The use of VRF within RLS is essential for learning the key features of the plant as it changes and for facilitating the ability of DDRCAC to readapt to the time-dependent plant dynamics.

DDRCAC was demonstrated for step and harmonic command following with noisy sensor measurements. Illustrative examples were presented to illustrate DDRCAC. In addition, DDRCAC was applied to a hypersonic aircraft model that transitions from MP to NMP. For this system, DDRCAC was able to follow step and harmonic commands despite the unknown transition from MP to NMP. For all three examples, DDRCAC was applied with the same tuning

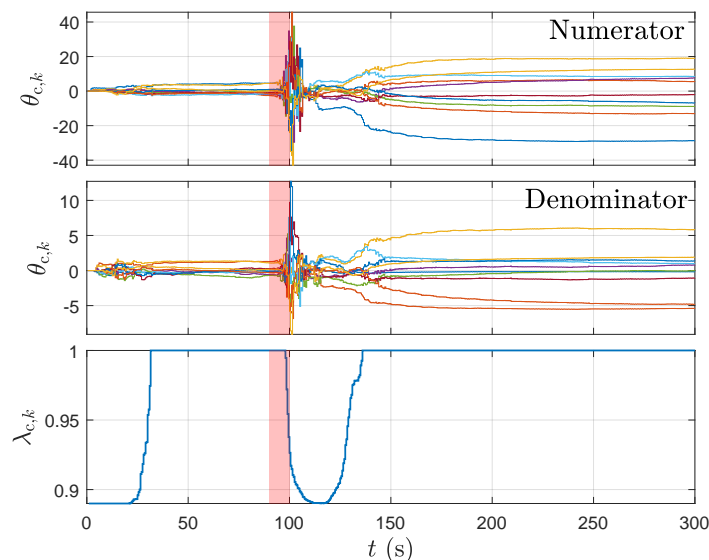


Fig. 13 Example 3: Numerator and denominator coefficients of the adaptive controller, and the control forgetting factor $\lambda_{c,k}$. Forgetting occurs for initial adaptation and the transition from MP to NMP.

hyperparameters.

Funding Sources

This research was supported by ONR under BRC grant N00014-18-1-2211.

Acknowledgments

We wish to thank John Burken and Tim Cox for providing the lateral aircraft dynamics model and helpful discussions.

References

- [1] Bolender, M., and Doman, D., "A Non-Linear Model for the Longitudinal Dynamics of a Hypersonic Air-breathing Vehicle," *AIAA Guid. Nav. Contr. Conf. Ex.*, San Francisco, CA, 2005.
- [2] Williams, T., Bolender, M., Doman, D., and Morataya, O., "An Aerothermal Flexible Mode Analysis of a Hypersonic Vehicle," *AIAA Atmospheric Flight Mechanics Conf. Ex.*, Keystone, CO, 2006.
- [3] Bolender, M. A., and Doman, D. B., "Nonlinear Longitudinal Dynamical Model of an Air-Breathing Hypersonic Vehicle," *AIAA J. Spacecraft Rockets*, Vol. 44, No. 2, 2007, pp. 374–387.
- [4] Rahman, Y., Xie, A., and Bernstein, D. S., "Retrospective Cost Adaptive Control: Pole Placement, Frequency Response, and Connections with LQG Control," *IEEE Contr. Sys. Mag.*, Vol. 37, 2017, pp. 28–69.
- [5] Buschek, H., and Calise, A. J., "Uncertainty Modeling and Fixed-Order Controller Design for a Hypersonic Vehicle Model," *AIAA J. Guid. Contr. Dyn.*, Vol. 20, No. 1, 1997, pp. 42–48.
- [6] Groves, K. P., Serrani, A., Yurkovich, S., Bolender, M. A., and Domand, D. B., "Reference Command Tracking for a Linearized Model of an Air-breathing Hypersonic Vehicle," *AIAA Guid. Nav. Contr. Conf. Ex.*, San Francisco, CA, 2005.
- [7] Parker, J., Serrani, A., Yurkovich, S., Bolender, M., and Doman, D., "Approximate Feedback Linearization of an Air-Breathing Hypersonic Vehicle," *AIAA Guid. Nav. Contr. Conf. Ex.*, Keystone, CO, 2006.
- [8] Jankovsky, P., Sigthorsson, D. O., Serrani, A., Yurkovich, S., Bolender, M., and Doman, D., "Output Feedback Control and Sensor Placement for a Hypersonic Vehicle Model," *AIAA Guid. Nav. Contr. Conf. Ex.*, Hilton Head, SC, 2007.

- [9] Sigthorsson, D., Jankovsky, P., Serrani, A., Yurkovich, S., Bolender, M., and Doman, D. B., "Robust Linear Output Feedback Control of an Airbreathing Hypersonic Vehicle," *AIAA J. Guid. Contr. Dyn.*, Vol. 31, No. 4, 2008, pp. 1052–1066.
- [10] Fiorentini, L., and Serrani, A., "Nonlinear adaptive control design for non-minimum phase hypersonic vehicle models with minimal control authority," *Proc. Conf. Dec. Contr.*, Shanghai, China, 2009, pp. 1405–1410.
- [11] Fiorentini, L., and Serrani, A., "Adaptive restricted trajectory tracking for a non-minimum phase hypersonic vehicle model," *Automatica*, Vol. 48, No. 7, 2012, pp. 1248 – 1261.
- [12] Sun, H., Yang, Z., and Zeng, J., "New Tracking-Control Strategy for Airbreathing Hypersonic Vehicles," *AIAA J. Guid. Contr. Dyn.*, Vol. 36, No. 3, 2013, pp. 846–859.
- [13] Xu, B., Huang, X., Wang, D., and Sun, F., "Dynamic Surface Control of Constrained Hypersonic Flight Models with Parameter Estimation and Actuator Compensation," *Asian J. Contr.*, Vol. 16, No. 1, 2014, pp. 162–174.
- [14] Rahman, Y., Aljanaideh, K., Sumer, E. D., and Bernstein, D. S., "Adaptive Control of Aircraft Lateral Motion with an Unknown Transition to Nonminimum-Phase Dynamics," *Proc. Amer. Contr. Conf.*, Portland, OR, 2014, pp. 2359–2364.
- [15] Ansari, A., and Bernstein, D. S., "Adaptive Control of an Aircraft with Uncertain Nonminimum-Phase Dynamics," *Proc. Amer. Contr. Conf.*, Chicago, IL, 2015, pp. 844–849.
- [16] Oppenheimer, M. W., and Doman, D. B., "Control of an Unstable, Nonminimum Phase Hypersonic Vehicle," Tech. rep., Air Force Research Laboratory, Wright-Patterson Air Force Base, OH, 2005. AFRL-VA-WP-TP-2005-304.
- [17] Xu, H., Mirmirani, M. D., and Ioannou, P. A., "Adaptive sliding mode control design for a hypersonic flight vehicle," *AIAA J. Guid. Contr. Dyn.*, Vol. 27, 2004, p. 829–838.
- [18] Parker, J. T., Serrani, A., Yurkovich, S., Bolender, M. A., and Doman, D. B., "Control-Oriented Modeling of an Air-Breathing Hypersonic Vehicle," *AIAA J. Guid. Contr. Dyn.*, Vol. 30, No. 3, 2007, pp. 856–869.
- [19] Shaughnessy, J. D., Pinckney, S. Z., McMinn, J. D., Cruz, C. I., and Kelley, M.-L., "Hypersonic vehicle simulation model: Winged-cone configuration," Tech. rep., NASA, NASA Langley Research Center, Hampton, VA, 1990. NASA-TM-102610.
- [20] Lennartson, B., and Soderstrom, T., "Investigation of the intersample variance in sampled-data control," *Int. J. Control*, Vol. 50, No. 5, 1989, pp. 1587–1602.
- [21] Shats, S., and Shaked, U., "Exact discrete-time modelling of linear analogue systems," *Int. J. Control*, Vol. 49, No. 1, 1989, pp. 145–160.
- [22] Osburn, S. L., and Bernstein, D. S., "An exact treatment of the achievable closed-loop H_2 performance of sampled-data controllers: from continuous-time to open-loop," *Proc. Conf. Dec. Contr.*, San Antonio, TX, 1993, pp. 325–330.